

DERIVATION OF MECHANICAL PROPERTIES FOR SAND

Leo Laine, ANKER – ZEMER Engineering AS, Norway
Andreas Sandvik, ANKER – ZEMER Engineering AS, Norway

Abstract

Mechanical properties for granular materials, such as sand, are important for accurate predictions of ground shock wave propagation and attenuation by use of an explicit solver. In the utilised material model the density dependence of both the longitudinal and shear (transversal) wave velocities, for a granular material, are accounted for.

Tri-axial compression tests with isotropic consolidation were performed on cylindrical specimens to obtain the porous equation of state ("EOS"). The longitudinal and shear wave velocities were measured at different pressure levels. As a result, the elastic loading and unloading bulk sound speed and shear modulus were derived. Additionally, tri-axial shear tests were performed at different pressure levels to obtain the pressure hardening yield surface.

Keywords: sand, equation of state, mechanical properties, shock waves, ground shock

1. Introduction

The Swedish Rescue Agency is the responsible authoritative for civil Rescue Centres and Shelters in Sweden. Rescue Centres are built and planned for accommodation of the civil defence command during preparedness and war. These buildings are constructed as one- or two storey buildings, and often, one floor is below ground surface. The framework is made of reinforced concrete.

Rescue Centres and shelters are not made 'hit proof' for cost reasons. They are just designed to resist conventional weapon loads that detonate at a certain distance from the structure. Air blast, debris, and ground shock are the typical weapon loads that are generated. Such loads can be calculated and taken into account in a hydrocode like AUTODYN™ [1].

Knowledge of the mechanical properties of the concerned soils on a macro level is significant for accurate prediction of ground shock propagation and attenuation. The saturation of soil is a very important factor for the transmission of the compressional wave in addition to the density and pressure dependence for the mechanical properties. In this article, mechanical properties for sand, from the village Sjöbo located in the southern part of Sweden, is described.

2. Tri-axial tests

The Norwegian Geotechnical Institute ("NGI") have both characterised the soil and performed tri-axial tests on the sand from Sjöbo [2]. The staff involved in the testing at NGI were Christian Madshus, Håkon Heyerdahl, and Toralv Berre.

2.1 Characterisation of soil

The grain size distribution in the sand was medium to coarse, with grain size number C_{60}/C_{10} approximately equal to 2 (two). The content of organic compounds was less than one percent. The in situ dry density was approximately $1574 \text{ [kg/m}^3\text{]}$; the average water content was approximately 6.57 percent. Finally, the average specific weight of the grains was $2641 \text{ [kg/m}^3\text{]}$.

2.2 Experimental set up

In the seven tests performed, two types of tri-axial cell devices were used. Firstly, the “NGI standard Cell device” [2] was used for tests up to 2 [MPa] in confinement stress, and secondly for tests above this confinement stress a rock triaxial cell device was utilised.

A cylindrical soil specimen with $h=90 \text{ [mm]}$ and $d=38 \text{ [mm]}$ in the rock tri-axial cell was enclosed in a rubber membrane inside the cell. By using a fluid in the chamber, the confining stress (pressure) equal to $\sigma_3 (= \sigma_2)$ was applied. The axial stress σ_1 was applied by a steel piston, which was employed by hydraulic pumps and a step motor.

The loading on the specimen was firstly isotropic consolidation ($P=\sigma_1=\sigma_2=\sigma_3$) with loading and unloading to different pressure levels, see Figure 1. Radial meter gauges were used to measure radial strain.

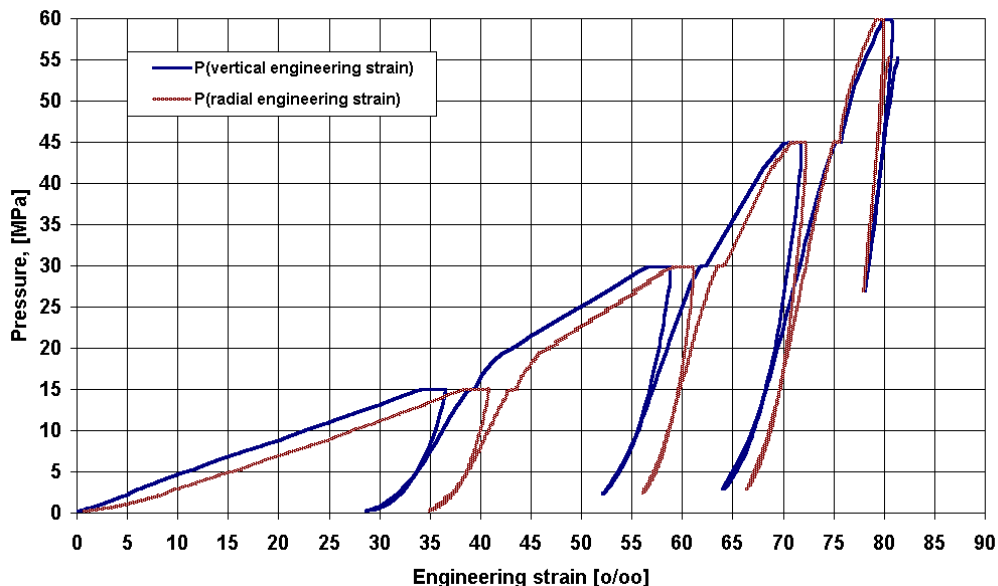


Figure 1: Test 847, maximum isotropic consolidation pressure $p_{\max} = 60 \text{ [MPa]}$.

From this part of the test, the EOS and the mechanical unloading bulk modulus, K_u , at different pressures levels can be derived.

After the isotropic consolidation, a shear test at different pressure levels, i.e. 2, 20, and 60 [MPa] were performed, see Figure 2. The radial stresses were kept constant (i.e. $\sigma_2 = \sigma_3 = \text{constant}$) while the axial stress was increased. Consequently, the maximum yield surface was established from the tests.

The “plastic yielding” that the Tri-axial shear tests showed see Figure 2, is mainly a structural collapse of a sand cylinder with size $H=2*D$ and can therefore be neglected in simulations of stress wave propagation as long as only moderate amount of sand grains are crushed, or phase transitions have not occurred.

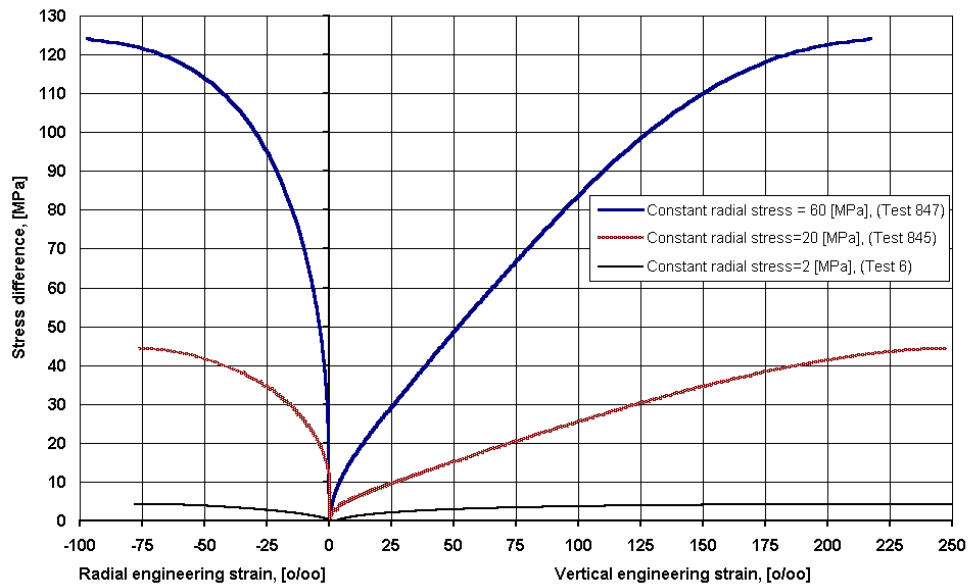


Figure 2: Tri-axial shear with three different constant radial stresses = 2, 20, and 60 [MPa] (Test 6, 845, and 847).

In the tests, where the rock tri-axial cell was employed, measurements of both the longitudinal wave (V_L) and the shear wave (V_S) were performed at different pressure levels. This was done both for the isotropic consolidation part and the shear part by using P- (i.e. longitudinal) and S- (i.e. transversal) wave transducers placed in the sockets on top and bottom of the samples. For tri-axial tests on soil, the standard method for volumetric strain determination is based on measuring the change in *pore water volume*. This was avoided since the measurement of V_L in water saturated soils are strongly influenced by the phase of the soil / water / gas matrix.

In Figure 3, results of V_L and V_S wave measurements are shown for test 847 and 848 during the isotropic consolidation. The measurements were made at the pressures 5, 10, 15, 30, 45 and 60 [MPa].

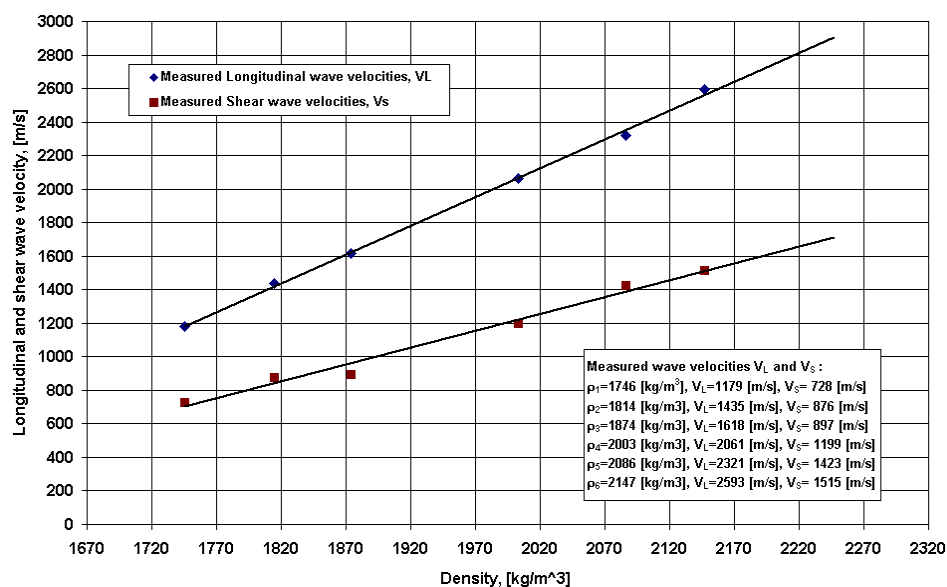


Figure 3: Measured Longitudinal and shear wave velocities at different pressures, 5, 10, 15, 30, 45, and 60 [MPa] (Test 847, 848).

In the NGI's standard tri-axial cell tests, *Bender Elements* [2] were used to measure the shear wave velocities. Consequently, accurate measurements were enabled from low pressures up to 2 [MPa].

3. Mechanical properties

The mechanical properties derived in this article were based on the *Granular material model*, implemented into AUTODYN™ [1]. This material model was developed to describe the compaction and the compaction wave of a porous material, [3].

3.1 Equation of state - Compaction

The EOS Compaction is described by a plastic compaction curve, which is given as a piecewise linear curve with ten points, namely density as a function of pressure, $P_i(\rho_i)$, as seen in Figure 4. The solid "asymptote" to this curve is linear:

$$P(\rho = \rho_{TMD}) = 0 \text{ and} \quad (1)$$

$$P = c_s^2 \cdot (\rho - \rho_{TMD}) \text{ with } \rho \geq \rho_{TMD}, \quad (2)$$

where

ρ_{TMD} : Theoretical Maximum Density (no porosity left), and

c_s : bulk sound speed of fully compacted material.

The elastic loading / unloading compaction curve is given by the density dependent bulk sound speed, $c(\rho)$:

$$P = c^2(\rho) \cdot \rho. \quad (3)$$

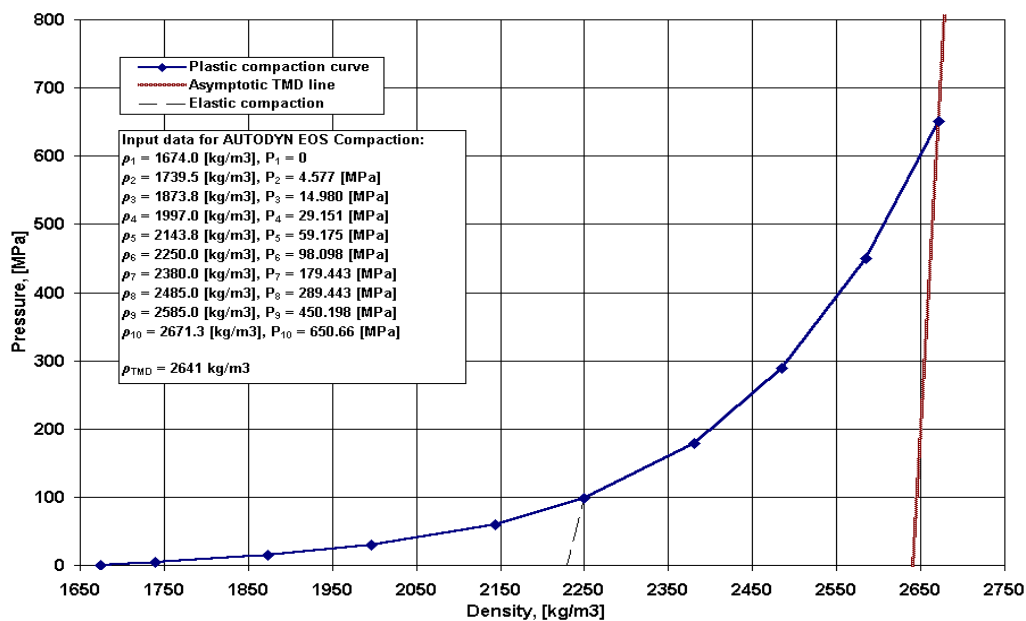


Figure 4: Input data for EOS Compaction of Sjöbo sand

The plastic compaction curve for pressures above 60 [MPa] was predicted by using a polynomial *best fit* of fifth order. The Theoretical Maximum Density was set equal to the average specific weight of the grains in the sand, 2641 [kg/m³].

The mineral content in the sand is similar what would be found in granite, thus the bulk sound speed of fully compacted material was derived from Shock Hugoniot Data for Westerly Granite [4]. The $c_s=4636$ [m/s] value was given by the two states ($\rho_0=2627$ [kg/m³], $P_0=0$) and ($\rho_1=3530$ [kg/m³], $P_1=19.394$ [GPa]).

From the longitudinal and shear wave velocity measurements the bulk sound speed, c , can be obtained from the following relationship in an isotropic, homogeneous media:

$$c = \sqrt{V_L^2 - \frac{4}{3} \cdot V_S^2}, \quad (4)$$

where

c : Bulk sound speed,
 V_L : Longitudinal wave, and
 V_S : Shear wave.

The longitudinal and shear wave velocities above the density 2150 [kg/m³] were predicted by using linear approximation.

The density dependent bulk sound speed, $c(\rho)$, was given as a piecewise linear curve of ten pairs, Figure 5.

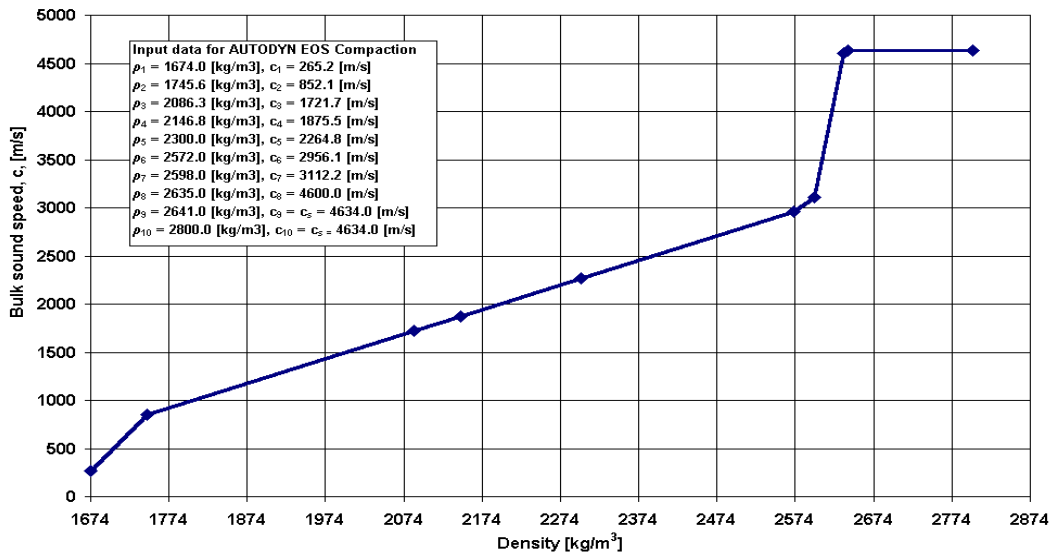


Figure 5: Input data for the density dependent bulk sound speed, $c(\rho)$ of Sjöbo sand

3.2 Strength Model – Granular

The yield surface in the Granular strength model is both density and pressure dependent, but here the only the pressure dependent part was utilised for description of the sand, i.e.:

$$Y(\rho, P) = f_1(\rho) + f_2(P), \quad \text{where } f_1(\rho) = 0. \quad (5)$$

In Figure 6 the utilised yield surface is shown as a function of pressure. The maximum stress difference from the tri-axial shear tests were utilised for determination of the maximum yield surface. For pressures above 102 [MPa], a linear approximation was utilised up to a maximum cut off value, which was set equal to the unconfined strength for Peaks Pike Granite [5].

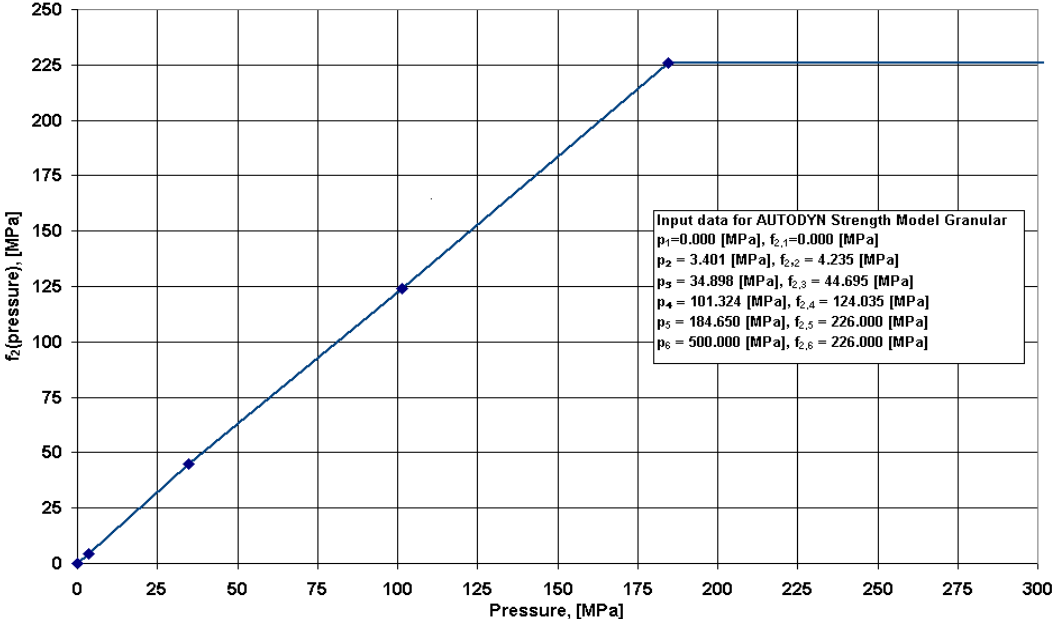


Figure 6: Input data for the pressure dependent yield surface, $Y=f_2(P)$ for Sjöbo sand.

The yielding in the Granular strength model is of Prandtl-Reuss type, and the shear modulus, $G(\rho)$, is defined to be density dependent. By use of the measured values of the shear wave velocities, the shear modulus was calculated from

$$G(\rho) = \rho \cdot V_s^2 \tag{6}$$

Input data for the density dependent shear modulus, $G(\rho)$, is shown in Figure 7.

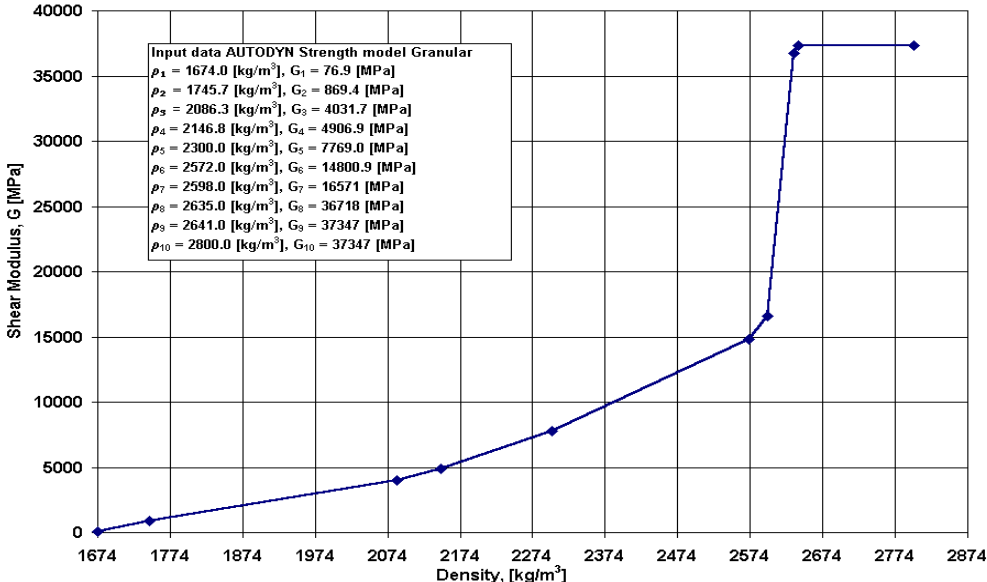


Figure 7: Input data pressure dependent Shear Modulus, $G(\rho)$, utilised for Sjöbo Sand.

3.3 Failure model –Hydro tensile limit

The failure model utilised for Sjöbo sand is the Hydro Tensile Limit, where a minimum pressure value, $P_{min} = -1e-3$ [Pa], was defined as failure criteria. This means when P_{min} is reached, the cell is not allowed to obtain shear stresses. The reheat option was also utilised, which allows the cell to reheat when the failed cell have positive pressure.

4. Numerical simulations of the shock wave in uniaxial strain state

If the shear strength is ignored in the considered material, the Rankine-Hugoniot relationships (i.e. conservation of mass, momentum, and energy) can be used to calculate the shock parameters for a material were a pressure, density, and energy discontinuity propagates, [6]:

$$\rho_0 \cdot U_s = \rho \cdot (U_s - U_p) \quad (7)$$

$$P - P_0 = \rho_0 \cdot U_s \cdot U_p \quad (8)$$

$$E - E_0 = \frac{1}{2} \cdot (P + P_0) \cdot (V_0 - V) \quad (9)$$

Equations (7)-(9) have five variables, pressure (P), particle velocity (U_p), shock velocity (U_s), specific volume (V=1/ρ), and energy (E). Consequently an additional equation is necessary to close the equation system. In this case the plastic compaction curve from the EOS will be utilised for the porous sand as seen in Chapter 3.1. This curve describes the pressure as a function of density and will be equivalent to the Hugoniot line.

By using equation (7) and (8), the shock wave velocity, U_s, and particle velocity, U_p, can be described as functions of pressure, P, and specific volume, V, i.e.

$$U_s^2 \cdot \rho_0^2 = \frac{P - P_0}{V_0 - V} \quad \text{or} \quad U_s = V_0 \sqrt{\frac{P - P_0}{V_0 - V}}, \text{ and} \quad (10a,b)$$

$$U_p^2 = (P - P_0) \cdot (V_0 - V) \quad \text{or} \quad U_p = \sqrt{(P - P_0) \cdot (V_0 - V)}. \quad (11a,b)$$

The shock wave will not follow the plastic compaction curve, i.e. the Hugoniot line, it will jump between the two states (P₀, V₀) and (P_i, V_i) on the plastic compaction curve by a straight line called the Rayleigh line. The slope of the Rayleigh line is proportional to the square of the shock wave velocity, U_s, as shown in equation (10a).

In Table 1, the shock wave variables, U_s and U_p have been calculated for the ten pairs, (P_i, V_i), which define the plastic compaction curve for the porous sand. The pressure P₀ equal to zero was used as initial state for every pressure discontinuity pair set, and the specific volume, V₀, was the inverse of the initial density, ρ₀ = 1674 [kg/m³].

Table 1: Calculated particle velocity, U_p, and shock wave velocity, U_s by eq. (10b) and (11b).

ρ _i [kg/m ³]	P _i [MPa]	U _p [m/s]	U _s [m/s]
1674	0.00	0.00	265.20
1739.5	4.577	10.15	269.47
1873.8	14.98	30.89	289.70
1997	29.15	53.07	328.12
2143.8	59.18	88.01	401.63
2250	98.10	122.48	478.45
2380	179.4	178.32	601.13
2485	289.4	237.55	727.87
2585	450.2	307.86	873.56
2671.3	650.7	380.94	1020.35

Table 2: AUTODYN-2D Results of shock wave variables ρ_i, P_i, and U_s when U_p is applied.

U _p [m/s]	ρ _i [kg/m ³]	P _i [MPa]	-U _s ^x [m/s]
-	-	-	-
10.1466	1739	4.57	270
30.8897	1874	15.0	290
53.0715	1997	29.1	328
88.0148	2144	59.2	402
122.482	2250	98.1	479
178.3197	2381	179.3	601
237.5478	2487	288.9	727
307.8598	2590	448.0	869
380.935	2671	650.4	1019

^xThe approximate shock wave velocity is based on arrival time, t_a, and the distance to studied target.

To simulate the plastic shock wave propagation in AUTODYN-2D with the Lagrange processor, the calculated particle velocities, U_p were utilised as boundary conditions on pipes with a length of 1 [m] filled with sand. 2000 cells were used in the wave direction. Convenient boundary conditions were applied so that uniaxial strain condition was achieved for the pipes.

In Table 2 the AUTODYN-2D results for the shock wave variables are shown for different particle velocities, U_p . By comparing the shock wave variables in Table 1 and Table 2, it is seen that there is an excellent agreement between the results.

In Figure 8 and Figure 9 the pressure wave propagation is shown for the four first particle velocities.

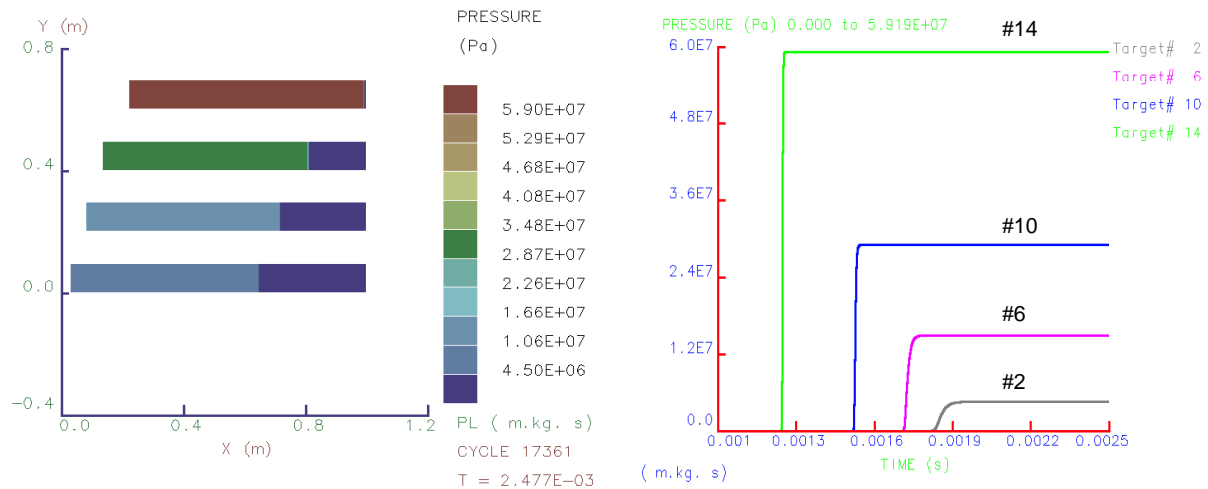


Figure 8: Pressure wave propagation at time 2.5 [ms] when $U_p = 10.15, 30.89, 53.07, \text{ and } 88.01$ [m/s]

Figure 9: Pressure time histories at 0.5 [m] when $U_p = 10.15$ (#2), 30.89 (#6), 53.07 (#10), and 88.01 (#14) [m/s].

The elastic unloading wave in the AUTODYN analysis is based on the actual bulk sound speed $C_i(\rho_i)$, and the shear modulus $G_i(\rho_i)$. The elastic unloading wave velocity travels faster than the plastic compaction wave or shock wave, which leads to fast attenuation, and energy absorption, of the propagating wave in the not fully compacted material.

5. Conclusions

In this article we have shown a methodology that can be used to derive mechanical properties of sand for ground shock analysis.

Measurement of the shear wave velocity, V_s , showed both density and pressure dependence. The density dependence of the bulk sound speed, $C_i(\rho_i)$, and the shear modulus, $G_i(\rho_i)$ is accounted for in the utilised material model, but the pressure dependence for C_i and G_i will be further investigated by experiments.

In the future work it is planned to verify the polynomial plastic compaction curve (EOS) for high pressures. Consequently, the isotropic consolidation phase will be performed to higher static pressures in future experiments. Additionally, inverse flyer plates tests will be considered to verify the Shock Hugoniot Curve for pressures close to the solid asymptote [7].

6. References

- [1] AUTODYN, *Theory Manual, Revision 4.0*, Century Dynamics Inc., 1998.
- [2] Heyerdahl H., Madshus C., *EOS-data for sand, Triaxial tests on sand from Sjøbo*, Norwegian Geotechnical Institute, NGI, 20001157-1, 2000
- [3] Moxnes J. F., Ødegårdstuen G., Atwood A., Curran P., "Mechanical properties of a porous material studied in a high speed piston driven compaction experiment", *30th ICT*, 1999
- [4] Marsh S. P., *LASL shock Hugoniot data*, University of California Press, 1980
- [5] Goodman R. E., *Introduction to Rock Mechanics, 2. Ed.*, New York, Wiley, 1989
- [6] Meyers, M., A., *Dynamic Behaviour of Materials*, John Wiley & Sons, Inc., 1994
- [7] Riedel, W., *Beton unter dynamischen Lasten Meso- und makromechanische Modelle und ihre Parameter*, EMI-Bericht 6/00, Fraunhofer, Institut Kurzzeitdynamik, Ernst-Mach-Institut, 2000.